Terr. Atmos. Ocean. Sci., Vol. 21, No. 3, 477-484, June 2010 doi: 10.3319/TAO.2009.11.17.02(TH)

Array Observations for Long-Period Basin Ground Motions in the Taipei Region during the M 7.1 Eastern Taiwan Offshore Earthquake of 31 March 2002

Bor-Shouh Huang[1, *], Yi-Ling Huang [2], Shiann-Jong Lee[1], Chi-Hsuan Chen [3], Kou-Cheng Chen[1], Win-Gee Huang[1], and Shuhjong Tsao [3]

[1] Institute of Earth Sciences, Academia Sinica, Taipei, Taiwan, ROC
[2] Institute of Applied Geosciences, National Taiwan Ocean University, Keelung, Taiwan, ROC
[3] Central Geological Survey, Ministry of Economic Affairs, Taipei, Taiwan, ROC

Received 12 August 2008, accepted 17 November 2009

ABSTRACT

This paper tracks the time history and spatial variation of the long-period (1 - 10 sec) strong ground motions recorded in the Taipei basin during the magnitude 7.1 earthquake of 31 March 2002, offshore of eastern Taiwan. The two-dimensional ground motions of this event were reconstructed from 89 free-field strong motion records over an area of 40 square km in northern Taiwan. The observed basin ground motions show complex waveforms, extended durations and multiple propagation directions in later phases. The dominant basin ground motions are identified to shake in its radial directions after the S-wave arrivals. Within the analyzed period band, results show that seismic waves amplifications were observed inside the sedimentary basin and its major amplifications were located on the eastern edge, the thick sediment portion of the basin. Across the Taipei basin, large ground motions were still maintained at the Linkou Tableland. Employing moving-window and waveform stacking techniques to analyze array seismograms revealed that high amplitude later phases have lower apparent velocities than the incident S-waves and cross the basin in multiple directions. We interpret these long period later arrivals to be surface waves, which are generated by a body wave interacting with the thick soft sediment of basin.

Key words: Strong motion, Seismic array, Basin amplification

Citation: Huang, B. S., Y. L. Huang, S. J. Lee, C. H. Chen, K. C. Chen, W. G. Huang, and S. Tsao, 2010: Array observations for long-period basin ground motions in the Taipei region during the M 7.1 eastern Taiwan offshore earthquake of 31 March 2002. Terr. Atmos. Ocean. Sci., 21, 477-484, doi: 10.3319/TAO.2009.11.17.02(TH)

1. INTRODUCTION

The Taipei basin is a triangular-shaped, tectonically controlled basin. Its western border is delimited by the Shanchiao fault, which separates it from the Linkou Tableland. Its southeastern boundary is marked by the Taipei fault, across from which stand the Western Foothills, while its northern rim is bordered by the Tatun Volcano Group (Fig. 1). The ground surface of Taipei basin is almost flat and tilting gently to the northwest. The total area of the basin region is about 240 square kilometers with an altitude of less than 20 meters (Fig. 1). The geological structure inside the basin has the Quaternary sediments, unconformably overlying the Tertiary basement (Teng et al. 2001). The basement structure has been explored by a dense seismic reflection survey and a deep borehole drilling study (Wang et al. 1994; CGS 2001). It is deepest near the western edge, where the depth to basement is about 600 - 700 m. On the eastern side, the interface with the basement is flatter, with a more constant depth of around 100 - 200 m (Wen and Peng 1998). The stratigraphic formations of the Quaternary sediment layers are, from top to bottom, surface soil, the Sungshan Formation, the Chingmei Formation, and the Hsinchuang Formation. The Sungshan Formation is composed mainly of alternating beds of silty clay and silty sand, and covers almost the whole Taipei basin. The Chingmei Formation is a fan-shaped body of conglomerate deposits. The Hsinchuang Formation consists of bluish grey, clayey sand with some conglomerate beds (Wang and Lin 1987). Within

* *Corresponding author*
E-mail: hwbs@earth.sinica.edu.tw

basin sediments, shear wave velocities were estimated from 170 to 650 m sec^{-1} and jump to 1200 m sec^{-1} in the basement (Wen and Peng 1998). P-wave velocities were estimated from 450 to 3000 m sec^{-1} in the basin (Wen et al. 1995; Wen and Peng 1998). According to the large shear wave velocity contact across the basement interface (~ 600 m sec^{-1}), the trap of seismic waves inside the basin and the amplification ground motion in surface are expected.

Ground motion amplification inside a basin can be induced by its deep basin shape, shallow soft layering soil and focused seismic waves during its propagation from the epicenter (Frankel and Vidale 1992; Gao et al. 1996; Kawase 1996). The spatial variation of ground motions over a sedimentary basin has been studied using analytical and numerical simulations over more than two decades (Aki 1988). Numerical simulations are usually employed to predict basin ground motions to identify the origin of its spatial variation. Usually, limited strong motion data are employed to interpret wave propagation effects or complex deep structures (Furumura and Koketsu 1998; Graves et al. 1998). However, due to spatial aliasing of the data, uncertainties with regard to waveform fitting are difficult to evaluate from seismograms with station spacing greater than the signal wavelengths of interest. To investigate the basin ground motion in detail, dense array observations are necessary. Previous work using seismic data recorded from the 1999 Chi-Chi, Taiwan Earthquake (Huang 2000; Furumura et al. 2001) and some urban arrays (Koketsu and Kikuchi 2000; Frankel et al. 2001) have shown the importance of dense array observations to learn the seismic amplification and wave propagation inside a sedimentary basin.

The strong motion array data from the 21 September 1999, Chi-Chi, Taiwan earthquake provided the first case which reconstructs a 2-D seismic wave field for the discussion of rupture behavior of a large earthquake (Huang 2000). However, at that time, the strong motion stations of the Central Weather Bureau (CWB) seismic network (Shin 1993) was not sufficiently dense to reconstruct 2-D surface ground motions to investigate in detail the basin effects of this disaster earthquake. After the Chi-Chi earthquake, more than 100 instruments were installed at stations in urban Taipei. The spacing between stations is about 1.5 km, on average.

A major earthquake (location = 24.406°N, 122.210°E; depth = 37 km; M_w = 7.1 after USGS) occurred off the east coast of Taiwan at 0652 UTC 31 March 2002 (Fig. 2). This was one of the two nearby Taiwan earthquakes with a magnitude greater than 7 following the magnitude 7.6, 1999 Chi-Chi Taiwan earthquake. This event was well recorded by the strong motion instruments deployed in the Taipei area. Those records provided an opportunity to investigate in detail the wave propagation characteristics across a sedimentary basin.

The aim of this report is both to present the success in reconstructing seismic wave field in a sedimentary basin and to discuss its seismic wave propagation effects of the Taipei basin from a distant large earthquake.

2. DATA

In the Taipei area, the strong motion accelerometers of the CWB network are uniformly deployed in the basin area and sparsely distributed on surrounding rock sites. Most strong motion instruments are equipped with GPS to provide absolute timing. Some research-oriented strong motion stations, operated by the Institute of Earth Sciences, Academia Sinica (IESAS) equipped with the same type of accelerometers as the CWB network and GPS clocks are also installed.

The 31 March 2002, offshore earthquake was the first event, after the 1999 Chi-Chi earthquake, with magnitude greater than 7 and was thoroughly recorded by stations in Taipei region. This data set represents the densest strong ground motion observations of the Taipei basin from a single event. Eighty-nine free-field 3-component strong motion data sets were recorded within an area of 40 × 40 km square in northern Taiwan during this event (Fig. 2). After the origin time corrections for some non-absolute timing records using the same procedure used by Huang (2000), the network seismograms can be accurately displayed according to its epicenter distance. Figure 3a shows the radial-component of the velocities bandpass-filtered at 0.1 - 1.0 Hz. These seismograms display coherent waveforms during their long-period signals. The largest arrivals in this section were the S-wave and its early later arrivals. Due to the proximity of the stations, the recorded seismograms are quite well correlated. However, to examine the waveforms in detail, the amplification of S-wave later phases from two nearby stations located inside and outside of sedimentary basin are different and the shaking duration inside the basin is extended (Fig. 3b). In this study, all seismograms were employed by array techniques to identify propagation characteristics of ground motions inside the Taipei basin.

3. ANALYSIS AND RESULTS

To enhance the long-period seismic wave propagation characteristics, the recorded accelerograms were converted to velocity seismograms and used a band-pass filter with corner frequencies of 0.1 and 1.0 Hz, respectively for further analysis. It is found that the filtered long-period ground motions have major amplitudes in its horizontal directions. To analyze wave types of major ground motions and its relative amplitudes between stations, the trajectories of ground motion in the horizontal plane for consecutive 5 seconds intervals before and after its peak values are plotted in Fig. 4. The horizontal particle motions of each seismic station provide a clear indication of major ground motion in its radial component although some stations near the basin boundary

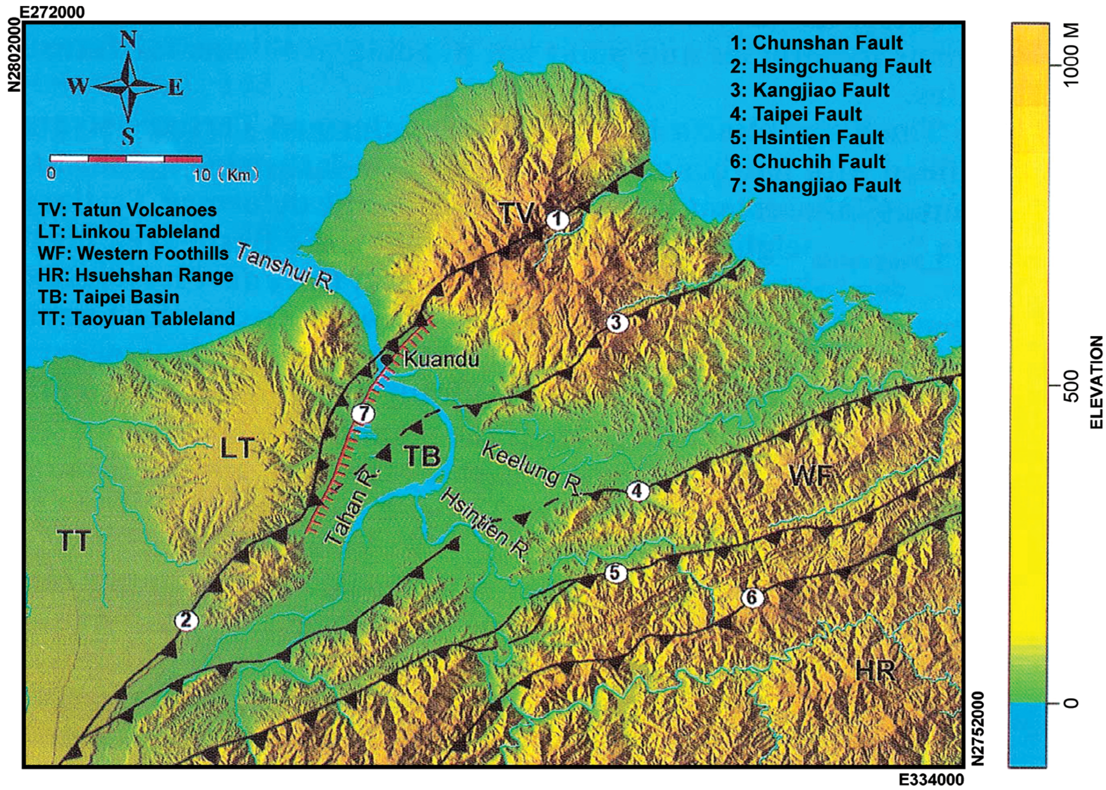

Fig. 1. Geomorphic features of the Taipei basin and its vicinity (modified from Teng et al. 2001). Color bar for elevation of the digital terrain is shown at the right.

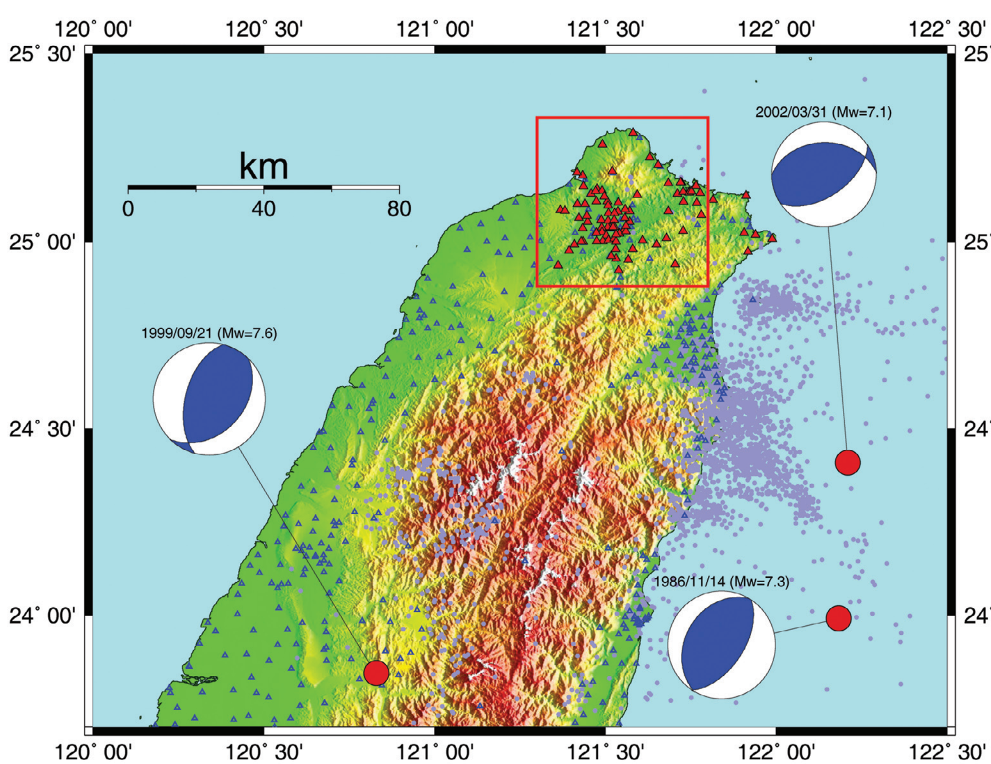

Fig. 2. Map of northern Taiwan and array configuration. The blue triangles represent the strong motion stations of the CWB seismic network. The red triangles (inside the red box) are stations used in this study. Epicenters (large red circles) and fault plane solutions of major events discussed in the study are also presented. Small blue dots represent one month's seismicity after the 31 March 2002 earthquake.

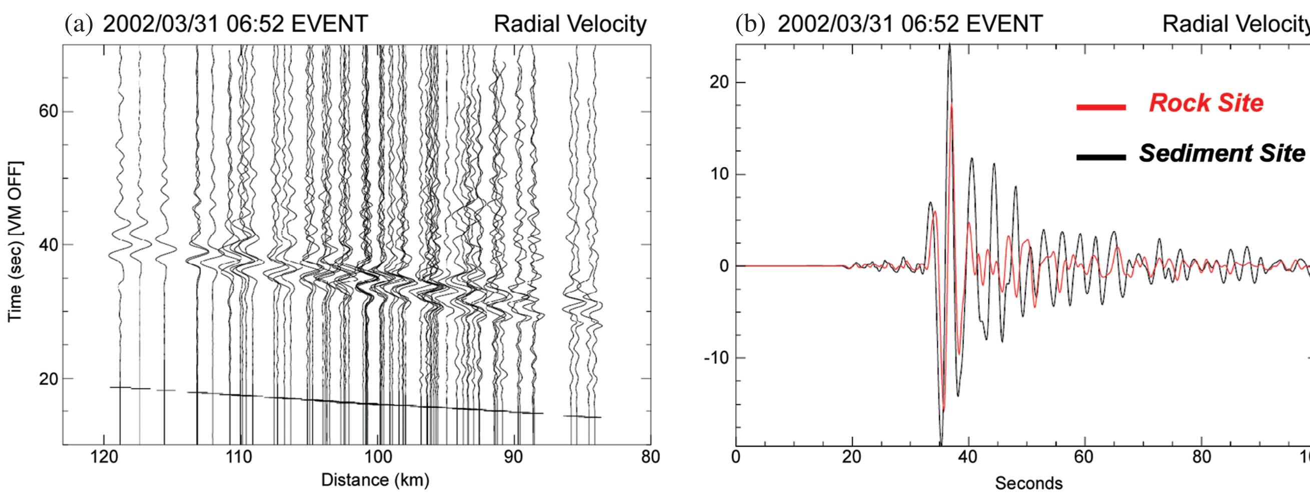

Fig. 3. (a) Record section for the 31 March 2002 event with a distance from 80 to 120 km. All seismograms are rotated to its radial direction, converted as velocities, filtered at 0.1 to 1.0 Hz, and plotted in the same scale. The vertical bar in each seismogram represents the picking for its first P-arrival time. (b) Comparing seismograms from a basin's deep soft sediment site (black trace) and its nearby rock site (red trace). The unit for amplitude scale is cm sec^{-1}.

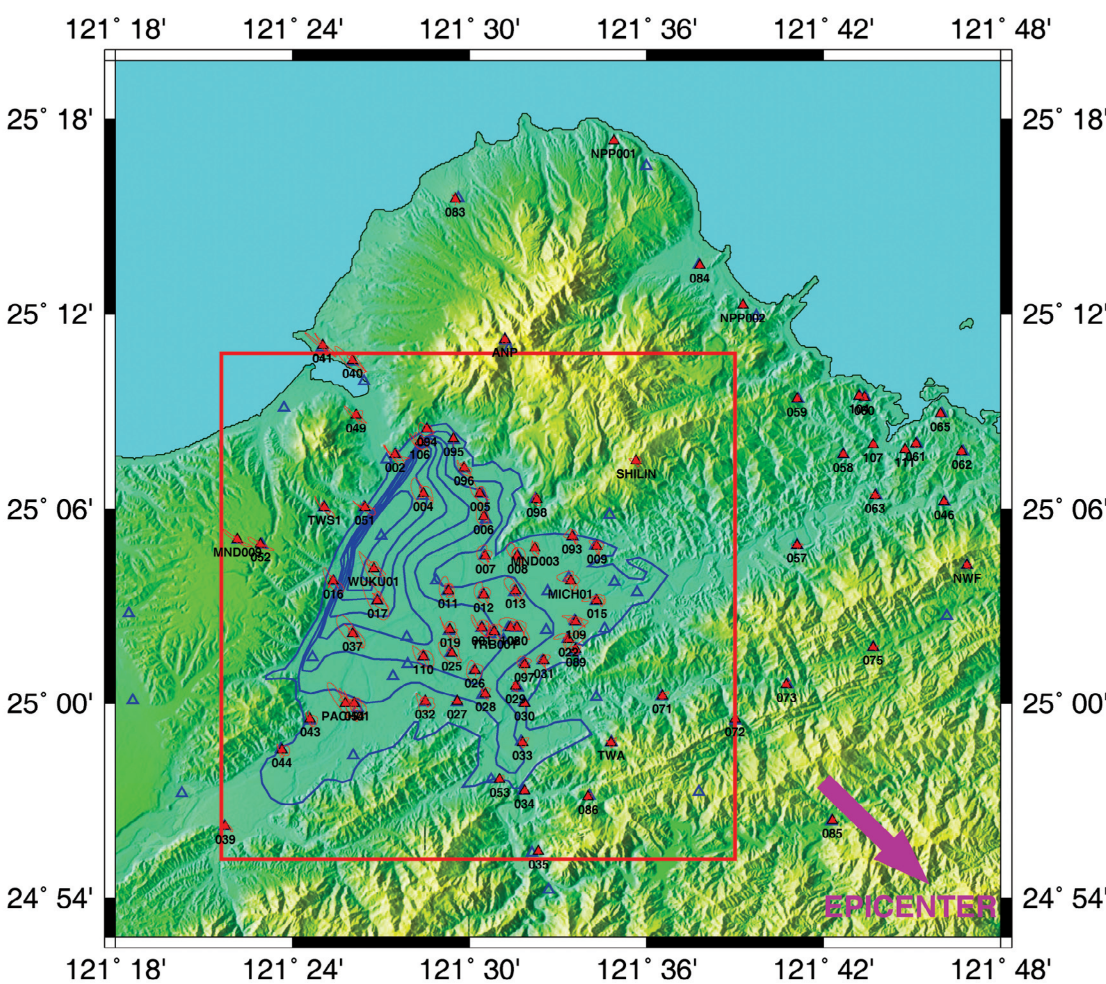

Fig. 4. Horizontal ground velocity particle motions of the 31 March 2002 event. The trajectories of ground motion are plotted at the locations of seismic stations and all particle motions are plotted in the same scale. The blue contour lines indicated the depth to the basin basement. Each line, from inner-most to outer-most, shows the depth of 100 m intervals from 600 m to the basin boundary (0 m), respectively. The large arrow indicates the direction to earthquake epicenter. The 2-D ground motion inside the red box region will be analyzed based on all array observations.

show relative variations with respect to its earthquake azimuth direction. The possible wave types of the filtered peak ground motions could be SV and/or Rayleigh waves. The spatial distribution of those trajectories also shows that the ground motions are significantly amplified in the sedimentary basin region of Taipei area and the major amplifications are found on its eastern edge and the covered deep sediment's western basin.

Following the wave field reconstruction procedure by Huang (2000), at each time step, the seismogram amplitudes are spatially interpolated to fill in an area as that marked in Fig. 4. To construct coherent snapshots of the long period wave field, in this study, the recorded accelerograms have been rotated to its radial and transverse directions to the source, then converted and filtered these as velocity seismograms. Figure 5 depicts the reconstructed wave field of this event at four times derived from the radial velocity seismograms (Fig. 3a). The snapshots show the radial-component first major pulse and its later phases to across this array clearly. According to the measurement based on the width of the color bands on the snapshots of Fig. 5, the dominant wavelength is determined to be near 10 km. The apparent wave propagation direction of the first major pulse can be estimated from these 2-D wave fields directly. The determined incident azimuth is consistent with the direction from earthquake source. Animation integrated by those snapshots showed both spatial and temporal variations of seismic wave amplitudes across Taipei basin, and provided a good opportunity to evaluate basin amplification from a larger earthquake occurred at eastern offshore of Taiwan. It is found that ground motion amplification within the Taipei basin was occurred first on its eastern boundary when S-waves hitting the basin. Then seismic waves were slightly decreasing its amplitudes when it propagated inside the basin. However, seismic waves increased its amplitudes and decreased its propagation speed as it crosses the thick

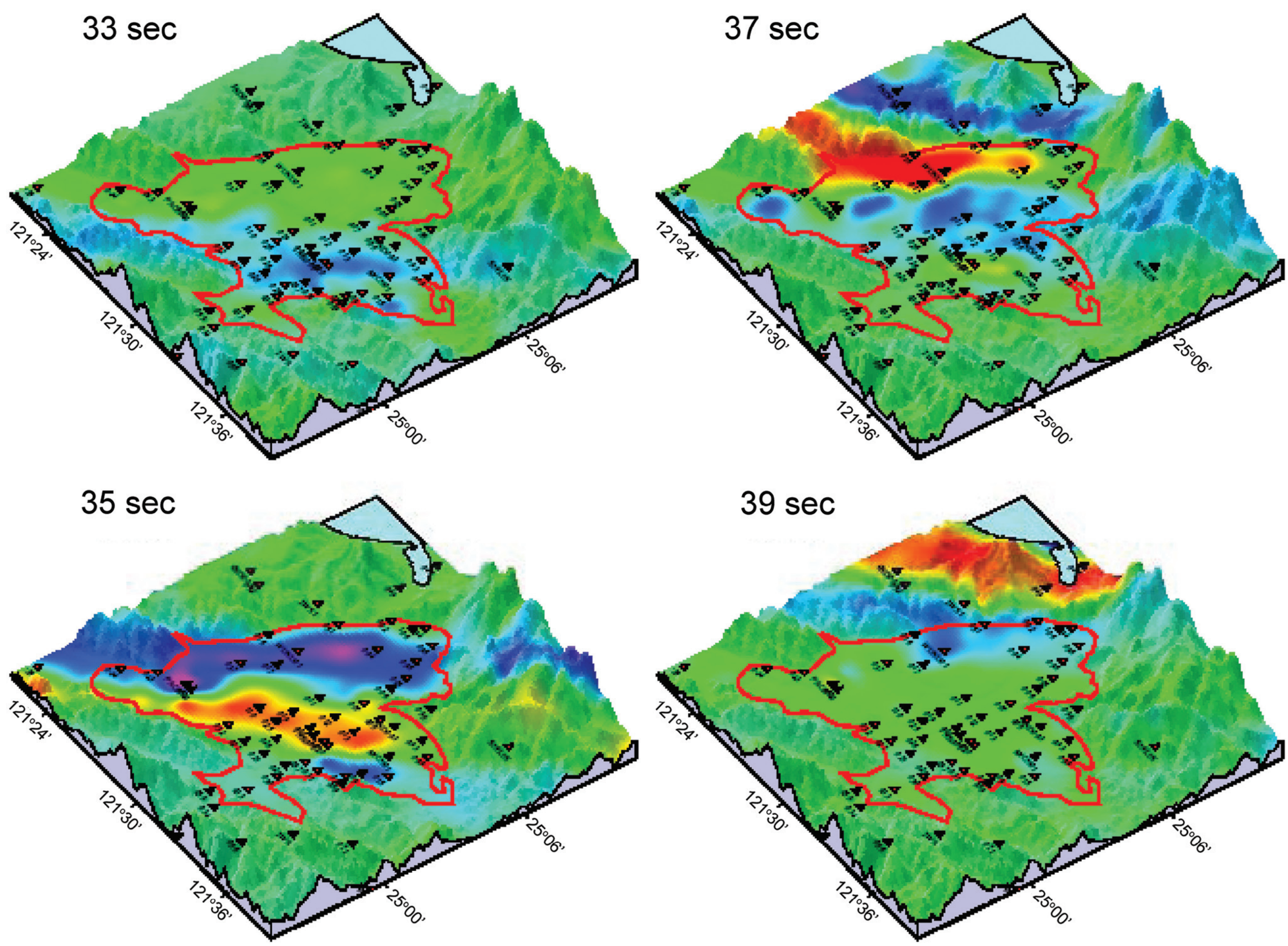

Fig. 5. Radial velocity ground motion snapshots show seismic wave propagation inside the Taipei basin and its surrounding area. The first snapshot, on the left at the top, was taken 33 sec after the onset of the source rupture. The succeeding panels were taken 2 sec apart. The red line on each panel represents the basin boundary. The snapshots were plotted using true amplitude and were clipped at 20 cm sec^{-1}. The amplitudes are scaled by color from blue to red for its low and high maximum, respectively.

sediment on the western side of basin. Past Taipei basin, it is found that the long period seismic waves kept its large amplitudes across the Linkou Tableland. Those features can be clearly seen also from the distribution of peak amplitude of those snapshots and as shown in Fig. 6.

To investigate this later phase in detail, a Beam-forming analysis (Huang 2001) is applied to examine the variations of propagation velocity and direction across this basin. According to the array waveform stacking procedure, the direction and slowness of seismic wave across an array can be determined in each selected time window. Analyzed results of this study show that the later phases have similar incident azimuths following the direct S-wave and show complex and multiple propagation directions in its later portion (Fig. 7). The apparent velocities are lower than the predicted incident S-wave (nearly 4.6 km sec^{-1} by the IASP91 model) and have values with 4.4 to 2.6 km sec^{-1}.

4. DISCUSSION AND CONCLUSIONS

Although the epicenter of the 31 March 2002 earthquake was nearly 100 km away from Taipei, this event has been reported to induce serious damage in some high-rise buildings near the basin boundary and widespread artificial structural injuries over the entire Taipei basin. In this study, within the analyzed frequency, the seismic amplifications inside the sedimentary basin are obviously greater than the surrounding basin area (Figs. 3 and 4). Reports for earthquake damage in the Taipei area were also found from the magnitude 6.8, 15 November 1986, eastern offshore Taiwan earthquake (Cheng et. al. 1999) and the 1999 Chi-Chi earthquake. However, the ground motions have induced different damage patterns for earthquakes from different azimuths approaching the Taipei basin. The origins of the ground motion amplification inside the Taipei basin appear to be induced by its deep basin shape, shallow soft layering soil or seismic wave focusing during its propagation from the epicenter (Yeh et al. 1988; Wen and Peng 1998; Chen 2003). However, due to limited seismic observations, its origin has been in long debate.

With the help of seismic data recorded by the dense seismic array in the northern Taiwan, an analysis of this study has demonstrated that the array aperture and instrument density are sufficient to allow reconstruction of the 2-D wave fields in the Taipei basin and its surrounding area. Indeed, not only the reconstructed wave fields can be presented by an individual snapshot to visualize the detailed seismic wave propagation inside the basin (Fig. 5) but also can be continuously displayed as an animated model. Herein, the reconstructed animation represents the time-dependent spatial ground motions across a sedimentary basin and provides immediate information of amplitude and propagating directions of incident seismic wave resonance inside the basin. Furthermore, these observations provide the unique opportunity to analyze the basin response in time domain because this kind of wave field evolution cannot be obtained

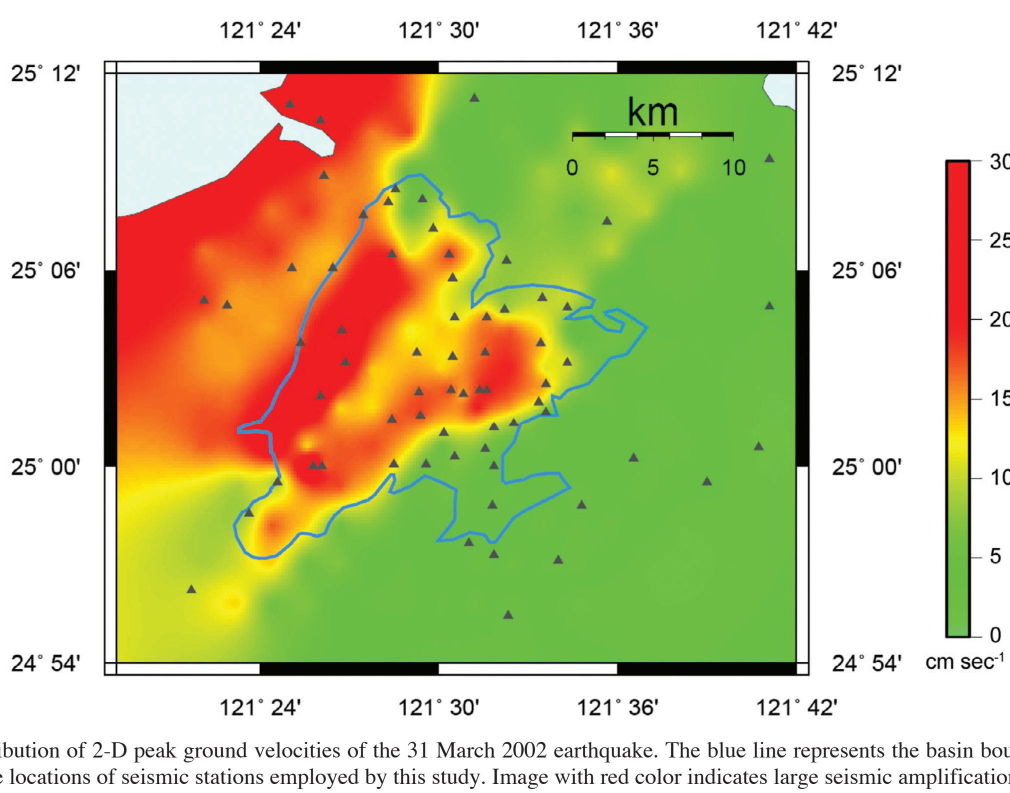

Fig. 6. The distribution of 2-D peak ground velocities of the 31 March 2002 earthquake. The blue line represents the basin boundary and symbol triangles indicate locations of seismic stations employed by this study. Image with red color indicates large seismic amplification.

from the traditional frequency domain spectrum analysis following Wen and Peng (1998).

Based on the reconstructed 2-D wave fields of this study, the propagation paths of those following direct S-waves later seismic phases can be visualized with ground motion animation. According to information on particle motion direction, wave propagation velocity and seismic amplification inside the basin obtained by this study, the later long period phases can be considered as basin induced surface waves. The basin amplifications induced by converted surface waves was proposed by Kawase (1996) to interpret the damage belt of the Kobe Japan earthquake and by Wen and Peng (1998) to predict seismic amplification of the Taipei basin. Results of this study support the prediction of amplification patterns of the Taipei basin by Wen and Peng (1998) and provide more detail about the energy transfer in spatial and temporal domains. The conclusion of this study suggests that during the 31 March 2002 earthquake, the long period basin amplification was induced by surface waves which were converted from basin trapped S-wave and its interaction with the thick soft sediment of basin.

Based upon this study, the reconstructed seismic wave fields can be considered as a new type of seismic data (3-D seismograms) and offer a potential application for the study

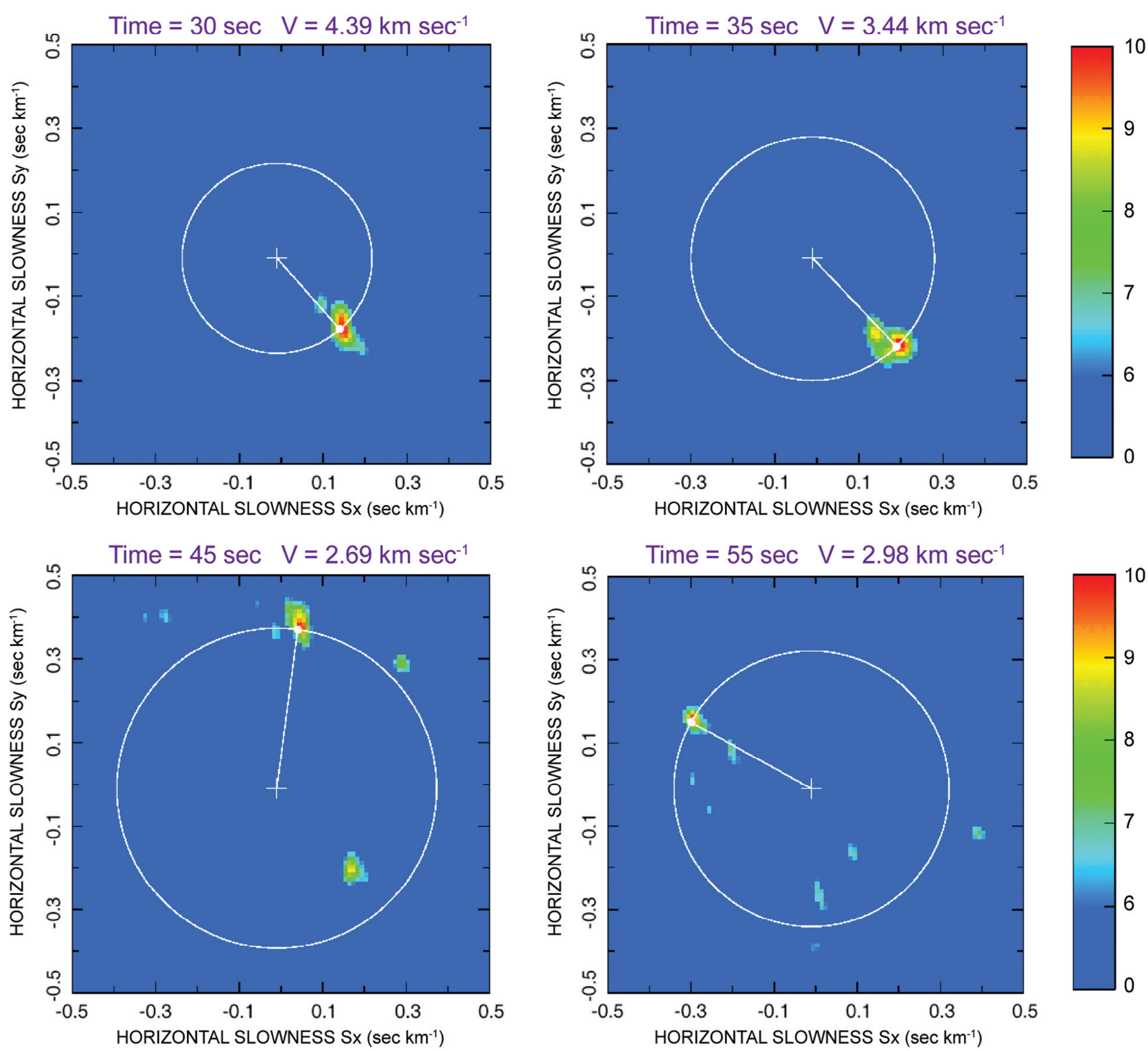

Fig. 7. Snapshots of stack seismic beams from successive windows of the 31 March 2002 event. Each seismic beam map represents the stacked peak values as a function of horizontal slowness in the east-western (Sx) and north-southern (Sy) directions, respectively. A window length of 5 seconds was used to construct each snapshot. Each window, the centroid time and determined apparent velocity are indicated in the top of each panel. The beam amplitude of each panel was normalized individually. The color bars at the right represent the relative intensity of those seismic beams. The determined peak of a seismic beam is shown as a white solid dot on each panel. The large circle on each panel represents the constant apparent velocity of the seismic waves across this array.

of basin amplification to greatly assist the development of wave propagation simulations based on 3-D numerical methods.

Acknowledgements The authors wish to express their appreciation to the Central Weather Bureau and the Institute of Earth Sciences, Academia Sinica for providing data used in this study. They also thank Profs. K. L. Wen, C. Y. Wang and T. L. Teng for their useful comments and valuable discussions. This study was supported by Academia Sinica and the National Science Council, ROC, under grants NSC96-2119-M-001-010, NSC96-2116-M-001-010, and CGS96-5226902000-01-02.

REFERENCES

Aki, K., 1988: Local site effects on strong ground motion. In: Von Thun, J. L. (Ed.), Earthquake Engineering and Soil Dynamics II: Recent Advances in Ground-Motion Evaluation, ASCE Geotechnical Special Publication, No. 20, 103-155.

CGS (Central Geological Survey), 2001: Annual report of Central Geological Survey, MOEA, Taipei, Taiwan, ROC, 171 pp.

Chen, K. C., 2003: Strong ground motion and damage in the Taipei basin from the Moho reflected seismic waves during the March 31, 2002, Hualien, Taiwan earthquake. *Geophys. Res. Lett.*, **30**, 1551, doi: 10.1029/2003GL017193. [Link]

Cheng, S. N., Y. T. Yeh, M. T. Hsu, and T. C. Shin, 1999: Photo album of ten disastrous earthquakes in Taiwan, Report of the Central Weather Bureau, 290 pp.

Frankel, A. and J. Vidale, 1992: A three-dimensional simulation of seismic waves in the Santa Clara Valley, California, from a Loma Prieta aftershock. *Bull. Seismol. Soc. Am.*, **82**, 2045-2074.

Frankel, A., D. Carver, E. Cranswick, T. Bice, R. Sell, and S. Hanson, 2001: Observations of basin ground motions from a dense seismic array in San Jose, California. *Bull. Seismol. Soc. Am.*, **91**, 1-12, doi: 10.1785/0120000071. [Link]

Furumura, M., T. Furumura, and K. L. Wen, 2001: Numerical simulation of Love wave generation in the Ilan Basin, Taiwan, during the 1999 Chi-Chi earthquake. *Geophys. Res. Lett.*, **28**, 3385-3388, doi: 10.1029/2001GL013114. [Link]

Furumura, T. and K. Koketsu, 1998: Specific distribution of ground motion during the 1995 Kobe earthquake and its generation mechanism. *Geophys. Res. Lett.*, **25**, 785-788, doi: 10.1029/98GL50418. [Link]

Gao, S., H. Liu, P. M. Davis, and L. Knopoff, 1996: Localized amplification of seismic waves and correlation with damage due to the Northridge earthquake: Evidence for focusing in Santa Monica. *Bull. Seismol. Soc. Am.*, **86**, S209-S230.

Graves, R. W., A. Pitarka, and P. G. Somerville, 1998: Ground-motion amplification in the Santa Monica area: Effects of shallow basin-edge structure. *Bull. Seismol. Soc. Am.*, **88**, 1224-1242.

Huang, B. S., 2000: Two-dimensional reconstruction of the surface ground motions of an earthquake: The September 21, 1999, Chi-Chi, Taiwan earthquake. *Geophys. Res. Lett.*, **27**, 3025-3028, doi: 10.1029/2000GL011481. [Link]

Huang, B. S., 2001: Evidence for azimuthal and temporal variations of the rupture propagation of the 1999 Chi-Chi, Taiwan Earthquake from dense seismic array observations. *Geophys. Res. Lett.*, **28**, 3377-3380, doi: 10.1029/2001GL012954. [Link]

Kawase, H., 1996: The case of damage belt in Kobe: "The basin-edge effect," constructive interference of the direct S-wave with the basin-induced diffracted/Rayleigh waves. *Seismol. Res. Lett.*, **67**, 25-34.

Koketsu, K. and M. Kikuchi, 2000: Propagation of seismic ground motion in the Kanto basin, Japan. *Science*, **288**, 1237-1239, doi: 10.1126/science.288.5469.1237. [Link]

Shin, T. C., 1993: Progress summary of the Taiwan strong motion instrumentation program. Symp. on the Taiwan strong motion instrumentation program, 1-10.

Teng, L. S., C. T. Lee, C. H. Peng, J. J. Chu, and W. F. Chen, 2001: Origin and geological evolution of the Taipei Basin, northern Taiwan. *West. Pac. Earth Sci.*, **1**, 115-142.

Wang, C. M. and T. P. Lin, 1987: The geology and land subsidence of the Taipei Basin. *Mem. Geol. Soc. China*, **9**, 447-464.

Wang, C. Y., C. Hsiao, and C. T. Sun, 1994: Reflection seismic stratigraphy in the Taipei basin (I) - Northwestern Taipei. *J. Geol. Soc. China*, **37**, 69-95.

Wen, K. L. and H. Y. Peng, 1998: Site effect analysis in the Taipei basin: Results from TSMIP network data. *Terr. Atmos. Ocean. Sci.*, **9**, 691-704.

Wen, K. L., L. Y. Fei, H. Y. Peng, L. F. Liu, and T. C. Shin, 1995: Basin effect analysis from a dense strong motion observation network. *Earthq. Eng. Struct. Dyn.*, **24**, 1069-1083.

Yeh, Y. H., C. H. Chen, and T. L. Teng, 1988: Study on focusing of seismic wave energy in Taipei basin: I. A dynamic ray-tracing approach. Proc. CCNAA-AIT Joint Seminar on Res. and Application for Multiple Hazards Mitigation, Taipei, 107-120.